

Temperature insensitive hysteresis free highly sensitive polymer optical fiber Bragg grating humidity sensor

Getinet Woyessa,^{1,*} Kristian Nielsen,¹ Alessio Stefani,^{1,2} Christos Markos,^{1,3} and Ole Bang¹

¹Department of Photonics Engineering, Technical University of Denmark, DK-2800 Kgs. Lyngby, Denmark

²Institute of Photonics and Optical Science (IPOS), School of Physics, The University of Sydney, NSW 2006, Australia

³CREOL, The College of Optics & Photonics, University of Central Florida, 4000 Central Florida Blvd., Orlando, FL 32816, USA

*gewoy@fotonik.dtu.dk

Abstract: The effect of humidity on annealing of poly (methyl methacrylate) (PMMA) based microstructured polymer optical fiber Bragg gratings (mPOFBGs) and the resulting humidity responsivity are investigated. Typically annealing of PMMA POFs is done in an oven without humidity control around 80°C and therefore at low humidity. We demonstrate that annealing at high humidity and high temperature improves the performances of mPOFBGs in terms of stability and sensitivity to humidity. PMMA POFBGs that are not annealed or annealed at low humidity level will have a low and highly temperature dependent sensitivity and a high hysteresis in the humidity response, in particular when operated at high temperature. PMMA mPOFBGs annealed at high humidity show higher and more linear humidity sensitivity with negligible hysteresis. We also report how annealing at high humidity can blue-shift the FBG wavelength more than 230 nm without loss in the grating strength.

©2016 Optical Society of America

OCIS codes: (130.5460) Polymer waveguides, (060.3735) Fiber Bragg gratings, (060.2370) Fiber optics sensors.

References and links

1. K. Peters, "Polymer optical fiber sensors - A review," *Smart Mater. Struct.* **20**(1), 013002 (2011).
2. D. J. Webb, "Fiber Bragg grating sensors in polymer optical fibers," *Meas. Sci. Technol.* **26**(9), 092004 (2015).
3. H. Dobb, D. J. Webb, K. Kalli, A. Argyros, M. C. J. Large, and M. A. van Eijkelenborg, "Continuous wave ultraviolet light-induced fiber Bragg gratings in few- and single-mode microstructured polymer optical fibers," *Opt. Lett.* **30**(24), 3296–3298 (2005).
4. Z. Xiong, G. D. Peng, B. Wu, and P. L. Chu, "Highly tunable Bragg gratings in single-mode polymer optical fibers," *IEEE Photonics Technol. Lett.* **11**(3), 352–354 (1999).
5. A. Stefani, S. Andresen, W. Yuan, N. Herholdt-Rasmussen, and O. Bang, "High sensitivity polymer optical fiber-Bragg-grating-based accelerometer," *IEEE Photonics Technol. Lett.* **24**(9), 763–765 (2012).
6. J. Jensen, P. Hoiby, G. Emiliyanov, O. Bang, L. Pedersen, and A. Bjarklev, "Selective detection of antibodies in microstructured polymer optical fibers," *Opt. Express* **13**(15), 5883–5889 (2005).
7. G. Emiliyanov, J. B. Jensen, O. Bang, P. E. Hoiby, L. H. Pedersen, E. M. Kjaer, and L. Lindvold, "Localized biosensing with Topas microstructured polymer optical fiber," *Opt. Lett.* **32**(5), 460–462 (2007).
8. C. Markos, W. Yuan, K. Vlachos, G. E. Town, and O. Bang, "Label-free biosensing with high sensitivity in dual-core microstructured polymer optical fibers," *Opt. Express* **19**(8), 7790–7798 (2011).
9. N. G. Harbach, "Fiber Bragg gratings in polymer optical fibers," PhD Thesis, Lausanne, EPFL (2008).
10. C. Zhang, X. Chen, D. J. Webb, and G. D. Peng, "Water detection in jet fuel using a polymer optical fiber Bragg grating," *Proc. SPIE* **7503**, 750380 (2009).
11. C. Zhang, W. Zhang, D. J. Webb, and G. D. Peng, "Optical fiber temperature and humidity sensor," *Electron. Lett.* **46**(9), 643–644 (2010).
12. W. Yuan, L. Khan, D. J. Webb, K. Kalli, H. K. Rasmussen, A. Stefani, and O. Bang, "Humidity insensitive TOPAS polymer fiber Bragg grating sensor," *Opt. Express* **19**(20), 19731–19739 (2011).

13. C. Markos, A. Stefani, K. Nielsen, H. K. Rasmussen, W. Yuan, and O. Bang, "High-Tg TOPAS microstructured polymer optical fiber for fiber Bragg grating strain sensing at 110 degrees," *Opt. Express* **21**(4), 4758–4765 (2013).
14. Z. F. Zhang and X. M. Tao, "Synergetic effects of humidity and temperature on PMMA based fiber Bragg gratings," *J. Lightwave Technol.* **30**(6), 841–845 (2012).
15. W. Zhang and D. J. Webb, "Humidity responsivity of poly(methyl methacrylate)-based optical fiber Bragg grating sensors," *Opt. Lett.* **39**(10), 3026–3029 (2014).
16. W. Yuan, A. Stefani, M. Bache, T. Jacobsen, B. Rose, N. Herholdt-Rasmussen, F. K. Nielsen, S. Andresen, O. B. Sorensen, K. S. Hansen, and O. Bang, "Improved thermal and strain performance of annealed polymer optical fiber Bragg gratings," *Opt. Commun.* **284**(1), 176–182 (2011).
17. B. T. Kuhlmeij, R. C. McPhedran, and C. Martijn de Sterke, "Modal cutoff in microstructured optical fibers," *Opt. Lett.* **27**(19), 1684–1686 (2002).
18. T. A. Birks, J. C. Knight, and P. S. Russell, "Endlessly single-mode photonic crystal fiber," *Opt. Lett.* **22**(13), 961–963 (1997).
19. A. Stefani, K. Nielsen, H. K. Rasmussen, and O. Bang, "Cleaving of TOPAS and PMMA microstructured polymer optical fibers: Core-shift and statistical quality optimization," *Opt. Commun.* **285**(7), 1825–1833 (2012).
20. A. Abang and D. J. Webb, "Demountable connection for polymer optical fiber grating sensors," *Opt. Eng.* **51**(8), 080503 (2012).
21. I. P. Johnson, D. J. Webb, K. Kalli, M. C. J. Large, and A. Argyros, "Multiplexed FBG sensor recorded in multimode microstructured polymer optical fiber," *Proc. SPIE* **7714**, 77140D (2010).

1. Introduction

The interest in polymer optical fibers (POFs) in sensing is steadily increasing because of their low processing temperature, high flexibility in bending, high fracture toughness, ease of handling, and non-brittle nature, which are properties that glass fibers do not have [1,2]. In addition, POFs are biocompatible and have a high elastic strain limit and low Young's modulus, which makes them advantageous for fiber Bragg grating (FBG) based strain and bio-sensing applications [3–8]. Some polymers, such as PMMA, are humidity sensitive and strongly absorb water [9–11], while other polymers, such as TOPAS, were shown to be insensitive to humidity [12,13]. Due to the moisture absorbing capability of PMMA based POFs, which leads to a change in the refractive index and size of the fiber, both of which contribute to a change in Bragg wavelength [9], they are used for developing humidity sensors [10,11]. Papers on PMMA POFBGs humidity sensors have so far reported different sensitivities to humidity and shown a strong dependence of the humidity sensitivity on the operating temperature and very low sensitivity at high temperature [14,15].

It is important to develop POFBG humidity sensors with a high sensitivity to humidity, no hysteresis in the humidity response and no cross-sensitivity to temperature. Likewise it is important to have a detailed knowledge of the humidity responsivity when designing all other types of POFBG sensors, in order to eliminate the cross-sensitivity to humidity. Here we address this issue by thorough characterization of PMMA mPOFBGs in a controlled environment in a climate chamber. It is well-known that prior annealing at a temperature close to, but below the glass transition temperature of the polymer, is important for stable and hysteresis free temperature and strain sensing with PMMA POFBGs [16]. Typically the recommended annealing temperature for PMMA POFBGs is around 80°C for more than 12 hours. At this temperature in a standard oven the relative humidity is very low, usually less than 10%. In prior investigations the humidity was thus low and not controlled during annealing. In this work, we demonstrate that humidity control during the annealing process of PMMA POFBGs plays a significant role in achieving high-quality humidity sensors that fulfil the above listed criteria and that in fact the relative humidity (RH) level during annealing should be high, preferable more than 90%.

2. Experiments and Results

To investigate the effect of humidity on annealing of PMMA mPOFs and the resulting humidity responsivity we prepared five identical 850 nm mPOFBGs using the phase mask technique. The fibers used in these experiments are PMMA mPOFs, from the same drawing,

fabricated at DTU Fotonik. The diameter of the fibers is 150 μm and the hole diameter and the pitch size are 1.5 μm and 4.2 μm , respectively. The hole to pitch ratio is 0.36 ensuring that the fiber is endlessly single mode [17,18]. A microscope image of the mPOF end facet, which was cleaved with a custom made cleaver at a temperature of 73°C of both blade and fiber [19], is shown as in Fig. 1.

We have conducted 5 series of experiments. In all experiments the PMMA mPOFBG was first connectorized with a single mode silica patch cable [20] and then placed in a climate chamber (CLIMACELL, MMM Group). A supercontinuum source (SuperK Compact, NKT Photonics) has been used as a light source and a spectrometer (CCS175 - Compact Spectrometer, Thorlabs) has been used to continuously track the peak of the grating during annealing in the climate chamber. Figure 1 shows the experimental setup for the humidity controlled annealing of PMMA mPOFBGs.

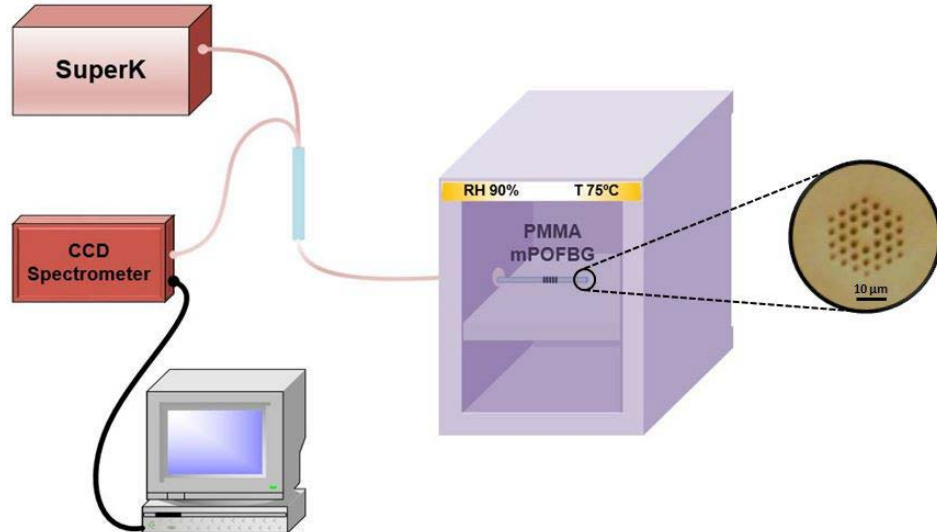


Fig. 1. Experimental setup for annealing and humidity response measurement of PMMA mPOFBGs. Inset: microscope image of the end facet of PMMA mPOF.

For all 5 experiments we first took the climate chamber to the ambient conditions, defined as 25°C and 50% RH and then carried out three annealing phases: pre-annealing, annealing and post-annealing. The pre-annealing phase consisted of 2 steps, in which the temperature and relative humidity were first kept at the ambient condition for two hours, after which the relative humidity was decreased to 10% at a fixed temperature of 25°C and kept there for three hours. The annealing phase always involved taking the temperature to 80°C and keeping it fixed at 80°C during a pre-determined relative humidity sequence. The post-annealing phase always consisted of taking the temperature and the relative humidity back to the ambient condition and keeping them there for 10 hours. Thus, for all 5 experiments, the annealing process was started and ended at ambient conditions. This precise control of initial and final state of the mPOFBG is extremely important in order to determine and compare the amount of blue-shift introduced by the five series of experiments without ambiguity. It is also very important that the post-annealing phase, after which sensitivity measurements were performed, always brought the mPOFBG to the same stable ambient condition (therefore the rather long post-annealing time of 10 hours), in order to be able to compare the relative humidity sensitivities measured in the five experiments.

For the first experiment the annealing phase was as follows: the temperature of the chamber was increased to 80°C, keeping the relative humidity at 10%. When the rate of blue-shift of the mPOFBG became less than 0.3 nm/hour, which we defined as mPOFBG

equilibrium condition, the RH of the chamber was increased to 30%. When the rate of blue-shift of the mPOFBG again became less than 0.3 nm/hour the RH of the chamber was increased to 50%, then to 70%, and 90%, each time when the mPOFBG reached equilibrium condition. The exact same experiment was then repeated with a new identical mPOFBG, but stopping the annealing phase at 70%, 50%, 30% and 10% RH, respectively. The results of the five humidity controlled annealing experiments are reported in Fig. 2.

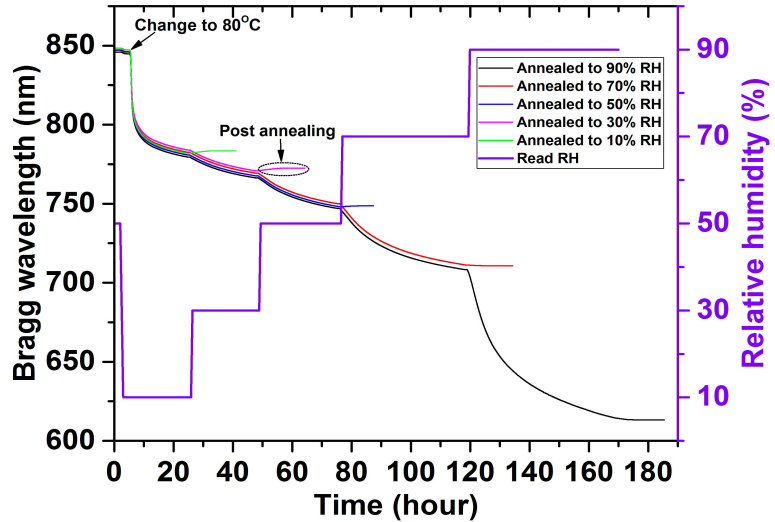


Fig. 2. Complete annealing process of PMMA mPOFBGs annealed at 80°C and up to a relative humidity of 90% (black), 70% (red), 50% (blue), 30% (pink) and 10% (green). The relative humidity sequence is shown only for the pre-annealing and annealing phases.

As it can be seen from Fig. 2, during the annealing phase the first rapid blue-shift is due to the temperature being increased from 25°C to 80°C (at fixed RH of 10%). This shows that initially the fiber was releasing the frozen-in stress induced during the fabrication process very fast. After 20 hours the blue-shift rate had decreased to 0.3nm/hour for all cases and the humidity was increased to 30% for the first four cases. It can be seen that as the RH was increased by 20%, the rate of blue-shift abruptly increased. This abrupt increase became higher the higher the RH level was and led to very large blue-shifts. Thus, for the higher RH levels, such as 70% and 90%, not only the rate of the blue-shift was faster but also the amount of the shift was larger. The total blue-shift for the mPOFBG annealed up to 90% was more than 230nm.

After each series of annealing experiment the humidity response of the mPOFBG sensor has been measured at three different temperatures: 25°C, 50°C and 75°C, in the interval of 10-90% RH, where the environmental chamber had greatest stability with a precision less than 0.3°C and 1% RH. For each temperature level, the humidity measurement has been done first by increasing the RH from 10% to 90%, with steps of 10% and then decreasing it from 90% to 10% with 10% steps. For both cases, the chamber was programmed to change the RH gradually over 30 mins and then to maintain the environmental conditions stable for 60 mins. Hence, the total time allowed before increasing or decreasing the relative humidity by 10% was 90mins. The response of the PMMA mPOFBG annealed to 90% RH for both increasing and decreasing relative humidity at 25°C is shown in Fig. 3(a). Figure 3(b) shows the comparison between humidity measurement at 25°C of the stabilized PMMA mPOFBGs that have been annealed to 90% and 10% RH.

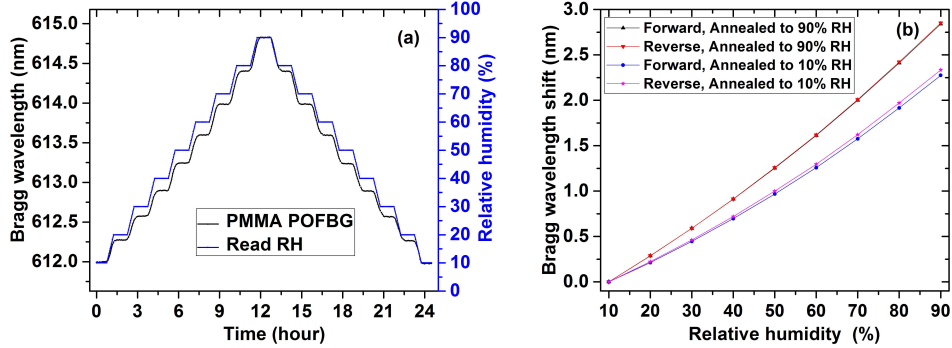


Fig. 3. (a) Measured humidity response at 25°C of PMMA mPOFBG annealed up to 90% RH versus time and humidity. The steps are defined in the text. (b) Corresponding stabilized response of the PMMA mPOFBGs annealed up to 90% and 10%.

The humidity sensitivity calculated by linear regression for the above humidity measurements are summarized in Fig. 4 for both increasing (circles) and decreasing (squares) humidity. The PMMA mPOFBG annealed up to 90% RH demonstrated the largest sensitivity to humidity, at all three temperature levels, while the one annealed only up to 10% RH had the lowest sensitivity.

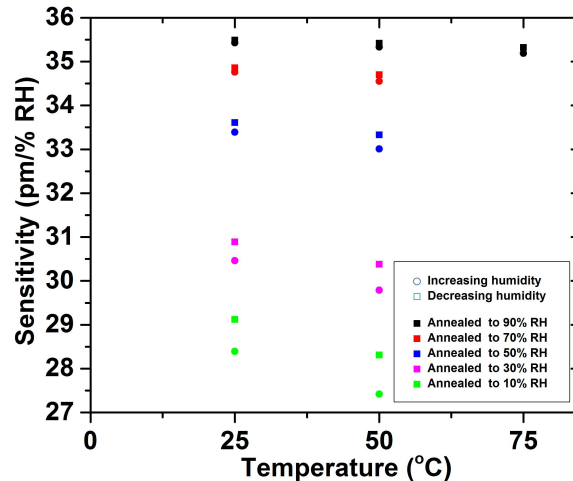


Fig. 4. Humidity sensitivity at 25°C and 50°C for PMMA mPOFBGs annealed to 90%, 70%, 50%, 30% and 10% RH and at 75°C for PMMA mPOFBG annealed to 90%.

The PMMA mPOFBG annealed up to 90% RH not only had the largest sensitivity, but also the lowest level of hysteresis, i.e., the smallest difference in sensitivity to humidity between the forward and reverse experiments. Importantly, the humidity sensitivity of the 90% mPOFBG is also to a good approximation temperature independent over the range of 25–75°C. From Fig. 4 it is important to notice that the hysteresis is considerably increased for mPOFBGs that have been annealed at lower levels of humidity. In addition these mPOFBGs annealed at low humidity also display a non-stable humidity response with a hysteresis that increases with operation temperature and a sensitivity that decreases with temperature.

At 75°C the PMMA mPOFBG annealed up to 90% measured a sensitivity of 35.19 ± 2.46 and 35.32 ± 2.54 pm/% RH, for increasing and decreasing humidity, respectively. Even at this

temperature the response thus to a good approximation hysteresis free. In contrast the other PMMA mPOFBGs annealed at a lower humidity showed a strong nonlinear decrease in the Bragg wavelength when the RH reached just above the annealing RH level as can be seen in Fig. 5. This showed that mPOFBGs annealed at low humidity or non-annealed mPOFBGs cannot be used for humidity sensing above a certain temperature level. Even if they were used only at low temperatures, their sensitivity to humidity is low, as seen in Fig. 4.

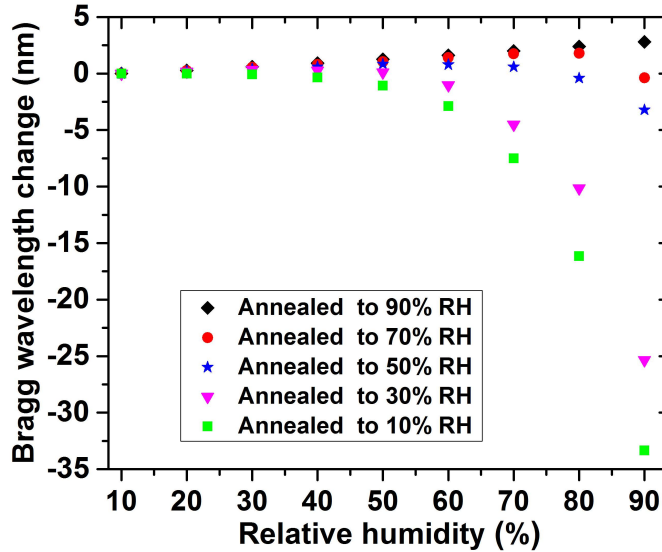


Fig. 5. Humidity responsivity at 75°C of PMMA POFBGs annealed up to 90%, 70%, 50%, 30%, and 10% RH.

In the above investigation and comparison between the performances of mPOFBGs annealed at different levels of humidity, we identified the mPOFBG annealed up to 90% RH as the one having the by far superior performance, i.e., the largest humidity sensitivity, the highest operation temperature, and the smallest hysteresis. The total annealing phase time of that mPOFBG was over 150 hours. Of course this can be shortened significantly by just directly annealing the mPOFBG at 90% RH and 80°C.

To demonstrate this we have done a sixth experiment. A new PMMA mPOFBG was inscribed at 850 nm in the same fiber type used for the above 5 series of experiments and annealed at constant 90% RH and 80°C, while tracking the Bragg wavelength. From Fig. 6(a) we see that the Bragg wavelength blue-shifted rapidly and took only about 24 hours to reach an equilibrium condition, which we defined earlier as when the rate of blue-shift has decreased to 0.3 nm/hour. It should be noticed that also in this case, coherently with the first experiment, the mPOFBG showed a permanent 235 nm blue-shift (in 24hours only), which is a record tuning of a POFBG without compromising the grating strength [21]. Figure 6(b) shows the amount of permanent blue-shift and strength of the PMMA mPOFBG recorded at ambient conditions before and after annealing at 80°C and 90% RH. This method of annealing at high humidity can therefore also be used to produce stable and strong gratings at short wavelengths where phase masks become more inefficient and expensive.

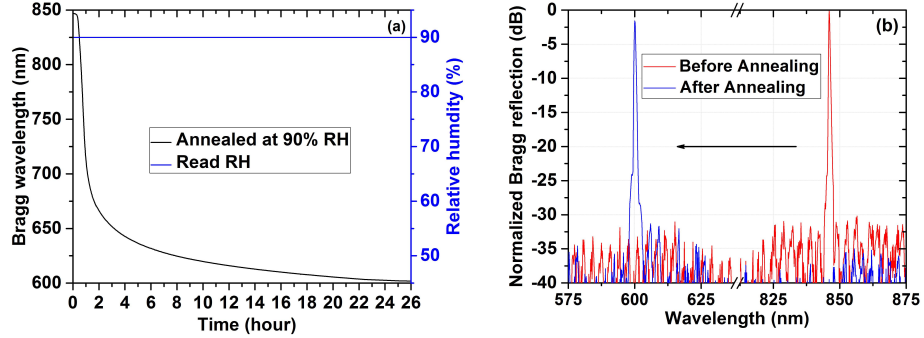


Fig. 6. (a) Annealing history of PMMA mPOFBGs annealed at 80°C and 90% RH. (b) Bragg reflection of PMMA mPOFBG before and after annealing at 80°C and at 90% RH both normalized to the non-annealed grating.

To test the responsivity of the annealed sensor humidity measurement has also been performed for this PMMA mPOFBG with the same procedure as used previously. For this PMMA mPOFBG the sensitivities returned by linear regression at 25°C, 50°C, and 75°C are 35.45 ± 2.58 , 35.31 ± 2.49 , and 35.17 ± 2.51 pm/%RH for increasing humidity and 35.50 ± 2.58 , 35.43 ± 2.50 , 35.28 ± 2.52 pm/%RH for decreasing humidity, respectively. These figures show that the humidity responsivities are in agreement with the mPOFBG annealed up to 90%RH in the early experiment. Therefore, by annealing a POFBG at fixed 90% RH and 80°C for only 24 hours it is possible to develop a stable humidity sensor that is able to operate between 25 and 75 °C in the range of 10-90% RH. The specific Bragg wavelength change versus increasing relative humidity at the three temperatures is plotted in Fig. 7.

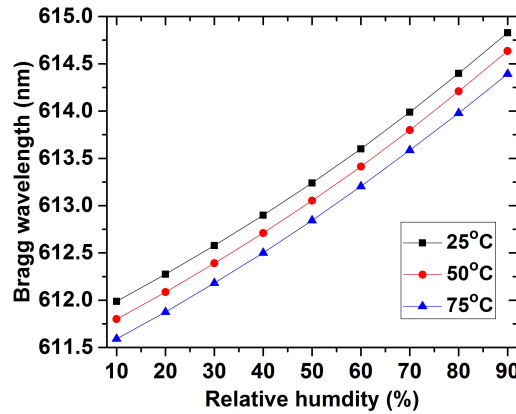


Fig. 7. Bragg wavelength change versus increasing in relative humidity at 25°C, 50°C and 75°C.

3. Conclusion

Our controlled annealing experiments have shown that when PMMA POFBGs are annealed at a given temperature and humidity the FBG wavelength shifts to the blue. The shift rate continuously decreases and eventually the shift stops. However, we have shown that when the humidity is again increased the blue-shift starts again at a higher rate than before and giving a larger total blue-shift. The rate increase and the total shift become larger with increasing

humidity. This shows that a high humidity level is very important in facilitating the annealing process.

PMMA POFBGs that are not annealed or annealed at a low humidity level have been shown to have low sensitivity to humidity and high hysteresis, particularly when operated at high temperature. PMMA POFBGs annealed at low humidity or not annealed therefore cannot be used for humidity sensing above a certain temperature level. Even if they are used at low temperature, they have a small sensitivity to humidity and high hysteresis. On the other hand, PMMA POFBGs annealed at high humidity (90% RH) have been demonstrated to have a superior response with a very low hysteresis, an improved sensitivity, and an increased stable operation temperature. PMMA POFBGs annealed at 80°C and 90% RH gave the same sensitivity, 35 pm/%RH, at 25, 50 and 75°C.

Finally, we have demonstrated that by annealing PMMA POFBGs for 24 hours at 80°C and 90% RH it is possible to tune the FBG wavelength, without loss in the grating strength, by a huge amount. This allows production of gratings at short wavelengths where POFs show lower loss but where the phase mask technique poses limitations in terms of efficiency and costs.

Acknowledgments

The research leading to these results has received funding from the People Programme (Marie Curie Actions) of the European Union's Seventh Framework Programme FP7/2007-2013/ under REA grant agreement n° 608382. The authors also acknowledge financial support from Innovation Fund Denmark for the project ShapeOCT (J. No. 4107-00011A), the Eugen Lommel Stipend for financial support and Danish Council for Independent Research (FTP Case No. 4184-00359B).